YMTHE, Volume *28*

Supplemental Information

Cardiac Nestin^{+} Mesenchymal Stromal Cells Enhance Healing of Ischemic Heart through Periostin-Mediated M2 Macrophage Polarization

Yan Liao, Guilan Li, Xiaoran Zhang, Weijun Huang, Dongmei Xie, Gang Dai, Shuanghua Zhu, Dihan Lu, Zhongyuan Zhang, Junyi Lin, Bingyuan Wu, Wanwen Lin, Yang Chen, Zhihong Chen, Chaoquan Peng, Maosheng Wang, Xinxin Chen, Mei Hua Jiang, and Andy Peng Xiang

Supplemental Figures and Legends

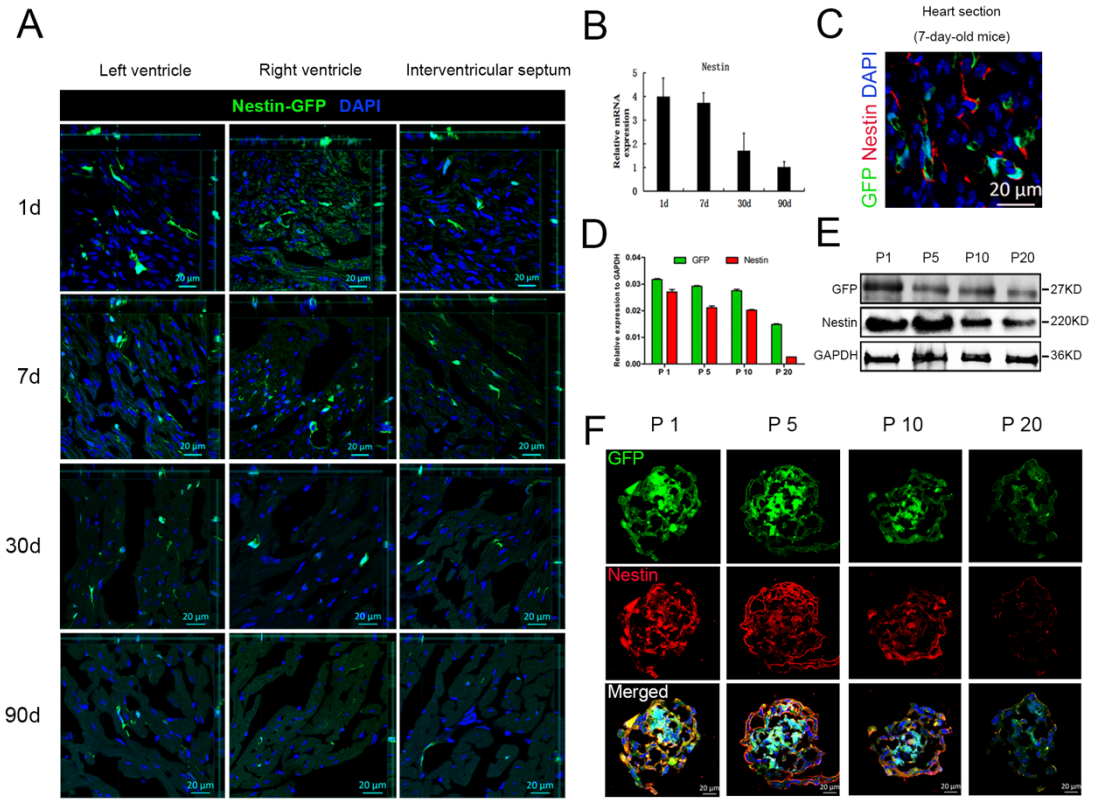

Figure S1. The spatial and temporal expression profiles of Nestin in the hearts of Nestin-GFP mice, and the co-expression of Nestin and GFP in Nes^{+}cMSCs following cell passage in vitro. (A) Distributions of Nestin-GFP-positive cells in the left ventricle, right ventricle, and interventricular septum of mouse hearts at postnatal days 1, 7, 30, and 90. **(B)** qPCR analysis showing that Nestin expression in the heart decreases with age. The Nestin mRNA levels were normalized with respect to those of GAPDH; n=5. **(C)** The expression and co-localization of GFP and Nestin in the heart tissues of 7-day-old Nestin-GFP reporter mice. Nestin was observed by staining with an anti-Nestin antibody. Scale bars, 20 μm. **(D)** The mRNA expressions of GFP and Nestin in Nes^{+}cMSCs of various passages (P1, P5, P10, and P20) were analyzed by qPCR; n=3. **(E and F)** The protein levels of GFP and Nestin were also analyzed by Western blotting (E) and the isolated GFP^{+} cells under clonal sphere-forming culture system co-expressed Nestin and GFP continuously, which were identified by immunofluorescence staining with anti-Nestin antibody (F). Scale bars, 20 μm. Data are shown as mean ± SEM.

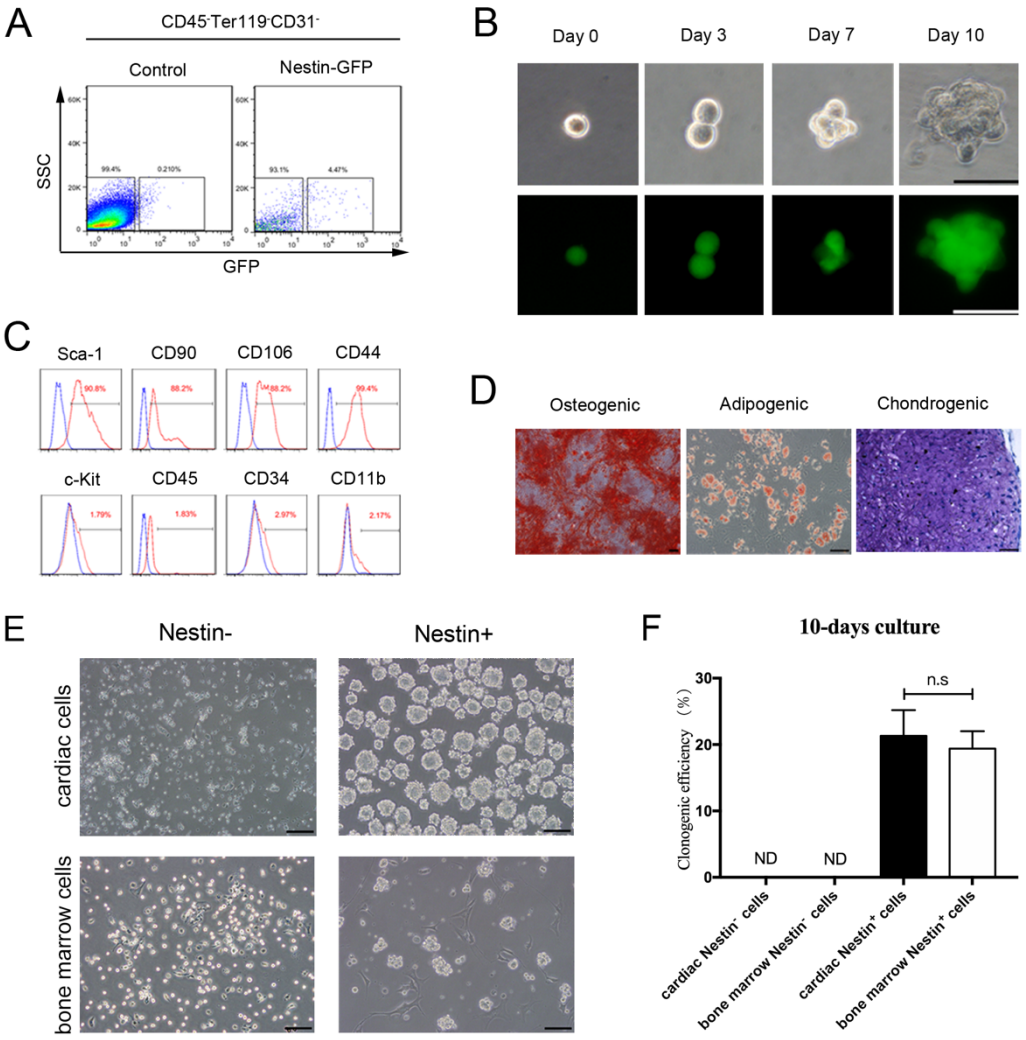

Figure S2. Isolation and characterization of Nestin-GFP$^+$ cells derived from mouse bone marrow. **(A)** Bone-marrow-derived CD45$^-$Ter119$^-$CD31$^-$ cells were flow cytometrically isolated from the bone marrow of 7-day-old Nestin-GFP transgenic mice, and Nestin$^+$ and Nestin$^-$ subpopulations were divided based on GFP expression. Cells from 7-day-old non-transgenic C57BL/6 mice were isolated as a control. **(B)** Representative images showing the clonal sphere growth of single Nestin-GFP$^+$ cells. Cells in the upper and lower columns were observed under bright and fluorescence field microscopy, respectively. Scale bars, 50 μm. **(C)** The expressions of some MSC-associated surface markers on Nestin-GFP$^+$ cells were detected by flow cytometry. **(D)** Representative stained images show that mouse bone-marrow-derived Nestin$^+$ cells could differentiate into osteocytes (Alizarin red), adipocytes (Oil red O), and chondrocytes (toluidine blue). Scale bars, 100 μm. **(E)** Freshly isolated heart- and bone-marrow-derived Nestin$^{+/-}$ cells were cultured in their respective serum-free complete media. After 10 days in culture, both Nestin$^+$ cell types yielded many clonal spheres, whereas their Nestin$^-$ counterparts remained as single cells. Scale bars, 100 μm. (F) A comparison of the sphere formation in wells containing a single cell showed that the clonogenic efficiencies (%) were similar in the cardiac and bone marrow Nestin$^+$ cells, Data are shown as mean ± SEM (n=5), ND =not detected, n.s. = not significant.

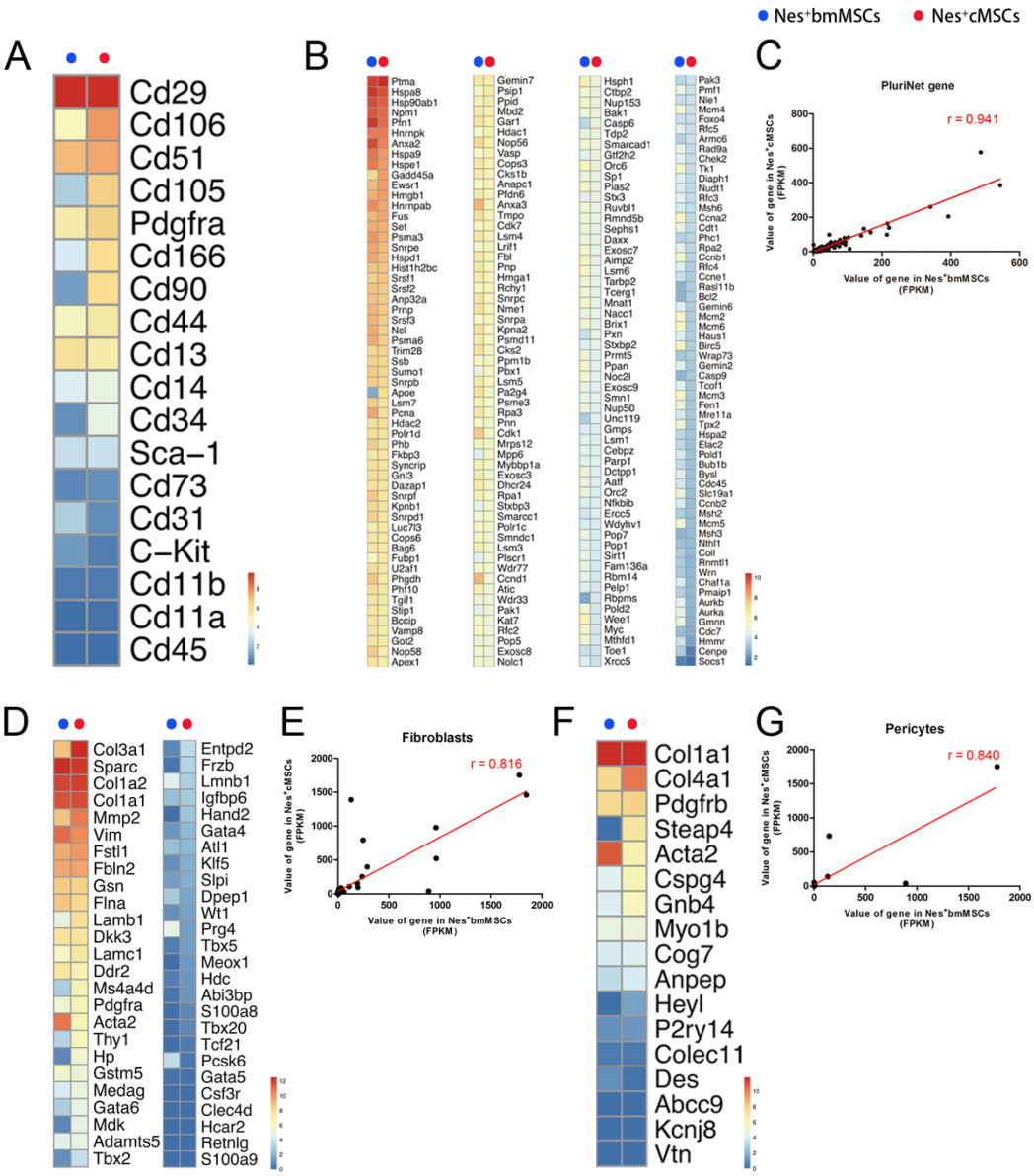

Figure S3. Transcriptional profiling reveals similar features of Nes^{+}cMSCs and Nes^{+}bmMSCs. (A) Heat map showing that the two types of MSCs had similar expression profiles for MSC-related surface marker-encoding genes. **(B and C)** Heat map of 230 PluriNet genes (~77% of the gene set) expressed in the two types of MSCs (FPKM>1), showing that both were in an active stem cell state (B) and had remarkably similar profiles (C, r=0.941, Pearson correlation coefficient). **(D and E)** Heat map showing that the two types of MSCs were very similar in terms of fibroblasts-related genes (r=0.816, Pearson correlation coefficient). **(F and G)** Heat map showing that the two types of MSCs were similar with respect to pericytes-related genes (r=0.840, Pearson correlation coefficient).

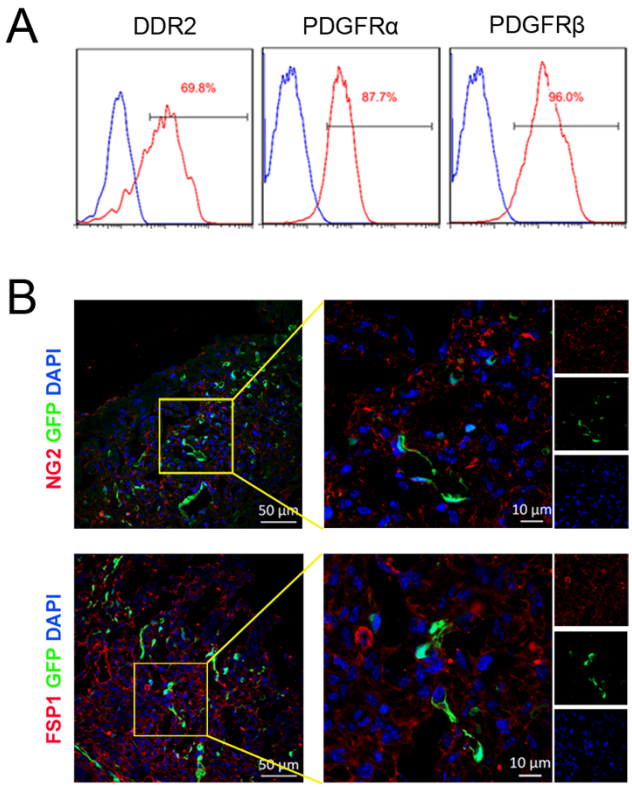

Figure S4. The fibroblast- and pericyte-related markers that are expressed by Nes^{+}cMSCs in vitro and in vivo. (A) Nes^{+}cMSCs express fibroblast (DDR2 and PDGFRα) and pericyte (PDGFRβ)-related cell surface markers, as analyzed by flow cytometry. **(B)** The co-localization of NG2 (a pericyte marker) and FSP1 (a fibroblast marker) with GFP in the heart of Nestin-GFP transgenic mice.

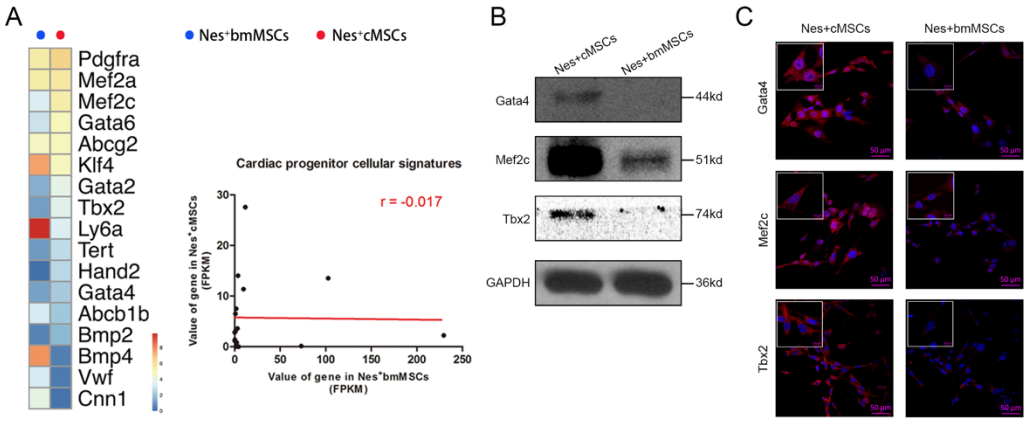

Figure S5. The expressions level of several cardiac transcription factors that expressed by Nes^{+}cMSCs were higher than that in Nes^{+}bmMSCs. (A) Heat map showing that the Nes^{+}cMSCs and Nes^{+}bmMSCs differed remarkably in terms of cardiac progenitor-related genes (r=0.017, Pearson correlation coefficient). (B and C) The protein levels of 3 cardiac transcription factors were analyzed by WB (B) and IF staining (C). Scar bar=50μm.

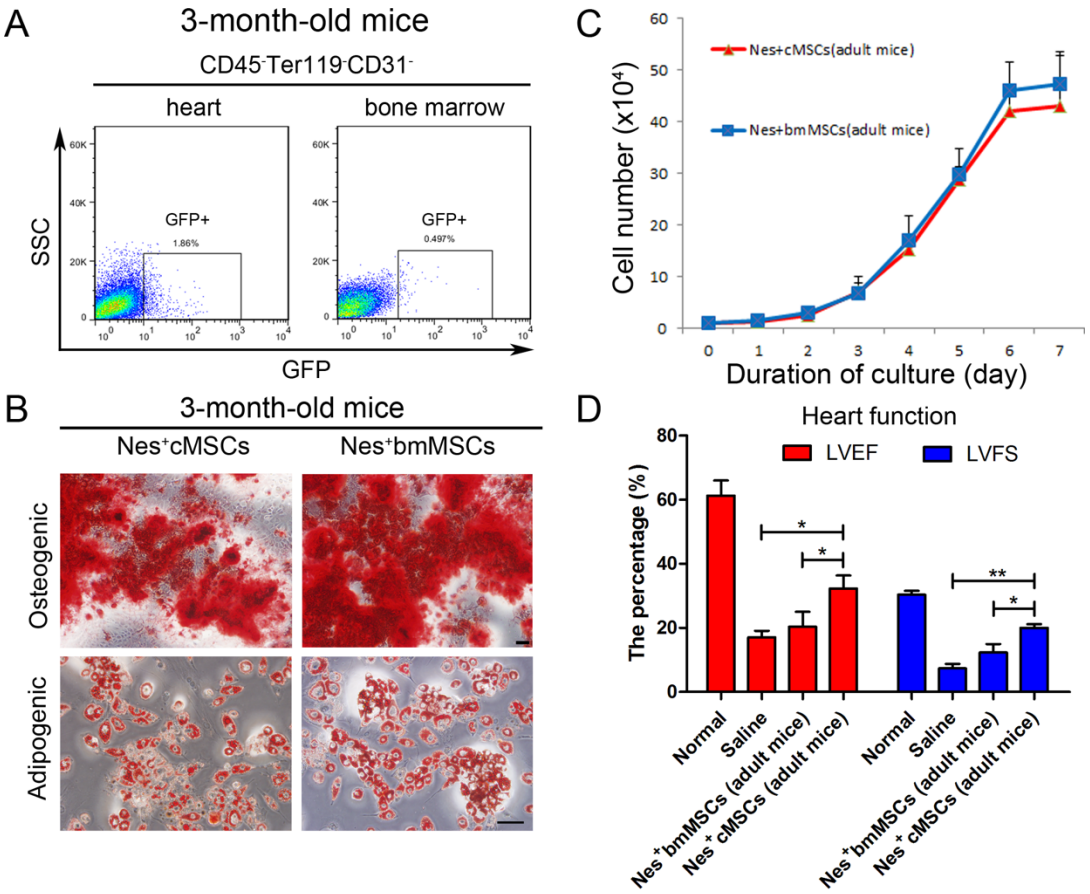

Figure S6. The Nes^{+}cMSCs cells, which were isolated from 3-month-old adult mice, still have stem cells property and cardioreparative effect on MI mice, compared with Nes^{+}bmMSCs group. (A) The Nes^{+}cMSCs and Nes^{+}bmMSCs from 3-month-old Nestin-GFP transgenic mice were freshly isolated by flow cytometry. GFP^{+} cells were isolated under the gate of CD45-Ter119-CD31- cells. **(B and C)** The two cells both have osteogenic and adipogenic potential when cultured in differential conditioned medium **(B)**; and the growth curve of the two adult mice-derived Nestin^{+} MSCs (Passage 10) were similar **(C)**. Scale bars, 100 μm. **(D)** Heart function was evaluated by echocardiography at 3 weeks post-AMI, and LVEF and LVFS were measured. *P <0.05, **P <0.01.

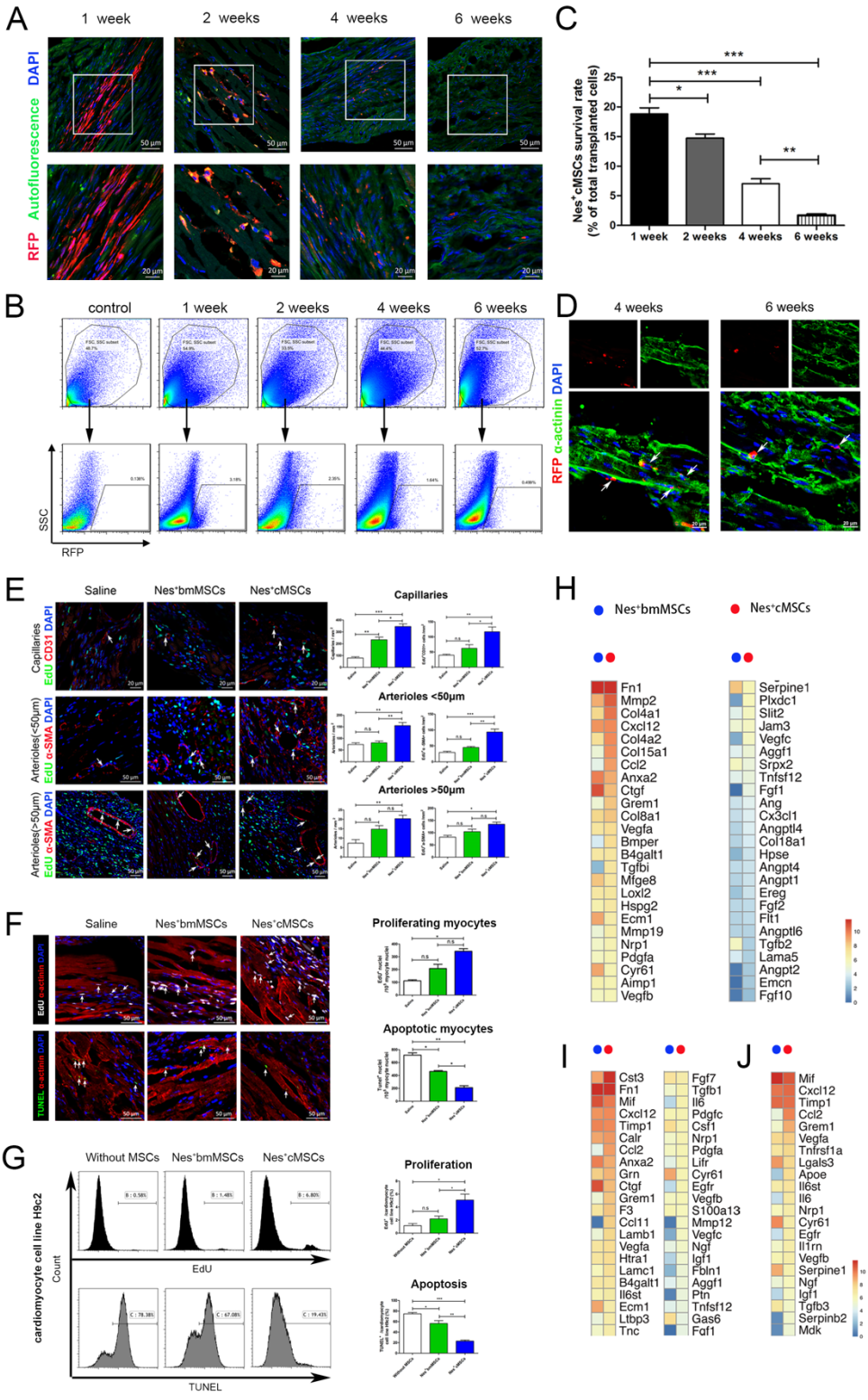

Figure S7. The long-term fate and cellular mechanisms of Nes^{+}cMSCs after transplantation post-AMI. (A) Representative images of RFP-Nes^{+}cMSCs persisting in hearts at 1, 2, 4, and 6 weeks after transplantation. **(B)** Representative flow cytometric plots of surviving RFP^{+} cells counted by fluorescence-activated cell sorting. Top gate indicates all cells isolated from the heart for flow cytometric analysis; bottom gate indicates the RFP^{+} cells sorted from the top gate. **(C)** The percentage of surviving RFP^{+} cells relative to the total transplanted RFP^{+}-Nes^{+}cMSCs at different time points; n=5. **(D)** Representative confocal images of no transdifferentiation of transplanted RFP-Nes^{+}cMSCs into cardiomyocytes at 4 and 6 weeks post-AMI. α-actinin indicates cardiomyocytes. **(E)** Representative

confocal images of capillaries and arterioles in the peri-infarcted myocardium 2 weeks post-AMI. $CD31^+$ indicates vascular endothelial cells, α-SMA^+ indicates vascular smooth muscle cells, and EdU^+ indicates the proliferation of cells. $CD31^+$ and α-SMA^+ cells positive for EdU are identified by white arrows (E). The numbers of capillaries, arterioles (<50 μm) and arterioles (>50 μm) in the saline, Nes^+cMSCs, and Nes^+bmMSCs groups were calculated (F); n=5. **(F)** Representative confocal images of cardiomyocytes in the peri-infarcted myocardium 2 weeks post-AMI. α-actinin$^+$ indicates cardiomyocytes, while EdU^+ and $TUNEL^+$ indicate cell proliferation and cell death, respectively. α-actinin$^+EdU^+$ and α-actinin$^+TUNEL^+$ cells are identified by white arrows. n=5. **(G)** The in vitro co-cultured experiment, the cardiomyocyte cell line H9c2 were subjected to 200 μM H_2O_2 for 6 h at the bottom, and then co-cultured with or without Nes^+cMSCs or Nes^+bmMSCs on the top of transwell system**,** and the percentages of proliferated and apoptotic H9c2 cells were quantified at 24 h by analyzing EdU and TUNEL signal through flow cytometry. **(H-J)** Heat map also shows that abundant of angiogenesis- **(H)**, proliferation- **(I)**, and anti-apoptosis-related gene **(J)** that were expressed by Nes^+cMSCs, rather than Nes^+bmMSCs. These genes were derived from Gene Ontology (GO) database, and genes with FPKM value more than one were enrolled into the analysis. Additionally, these genes profiles were derived from pre-transplanation of Nes^+cMSCs and Nes^+bmMSCs. *P <0.05, **P <0.01, ***P <0.001, and n.s. = not significant.

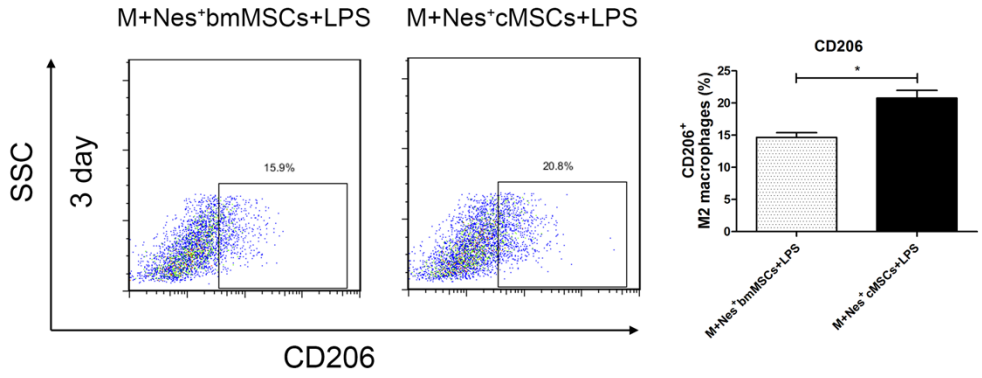

Figure S8. Nes^+cMSCs showed superior effect than Nes^+bmMSCs in inducing the polarization of M2 macrophages in vitro. The percentage of $CD68^+CD206^+$ M2 macrophages was analyzed by flow cytometry after macrophages were co-cultured for 3 days with Nes^+bmMSCs or Nes^+cMSCs; Data are shown as mean ± SEM; n=3. *P <0.05.

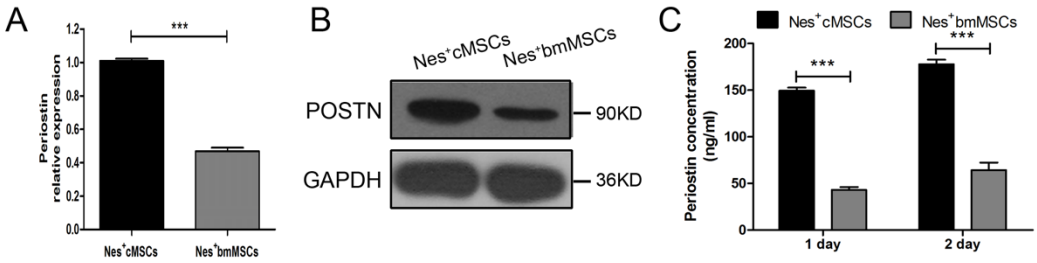

Figure S9. Nes^+cMSCs express and secrete higher Periostin than Nes^+bmMSCs. (A-C) The expressions level of Periostin between Nes^+cMSCs and Nes^+bmMSCs were analyzed at mRNA and protein level using qPCR (A), WB (B), and the Periostin protein in supernatant after 1 and 2 d culture was analyzed by ELISA (C). n=3. ***P<0.001.

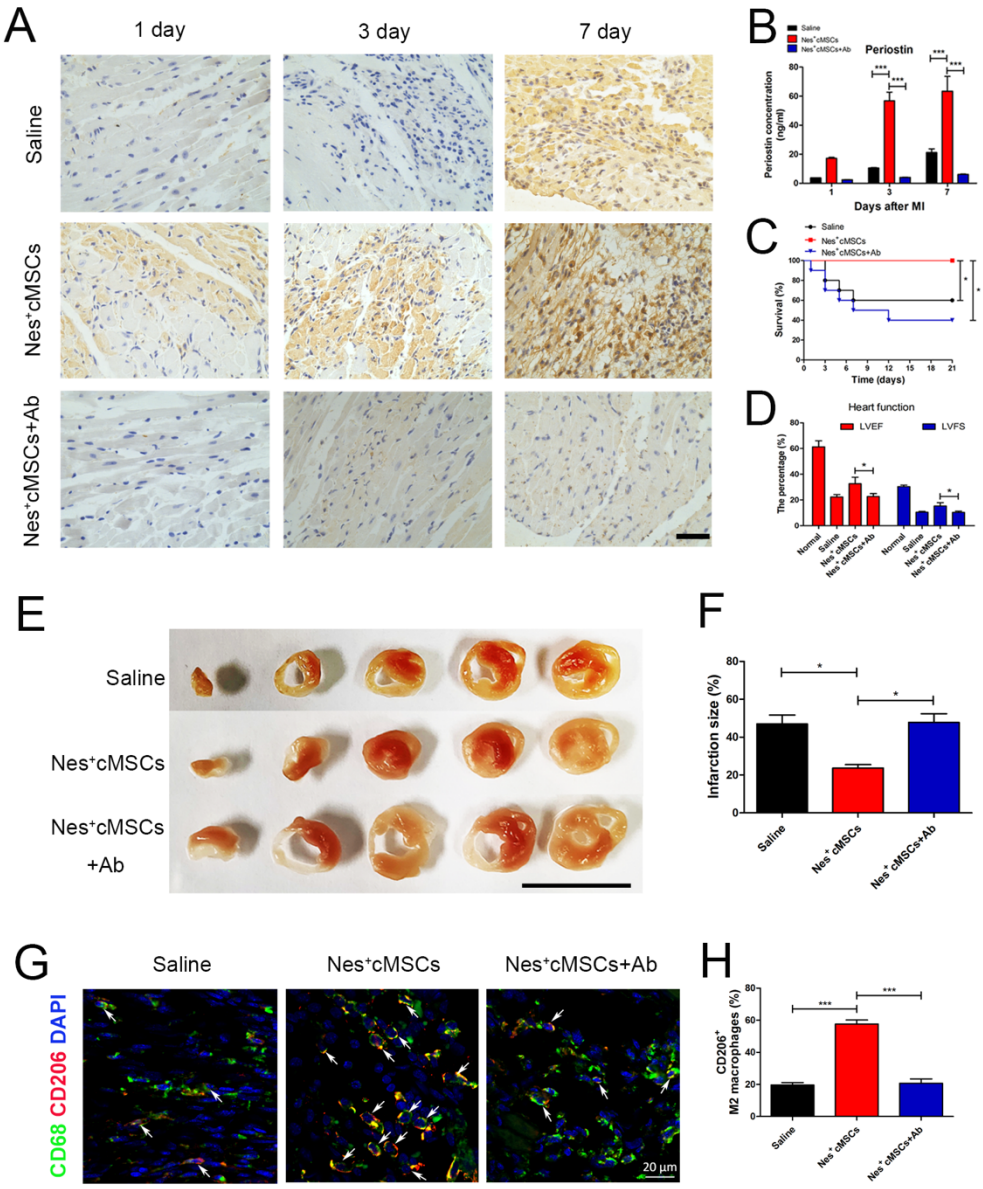

Figure S10. The neutralization of Periostin by a specific antibody attenuates the therapeutic effect of Nes^{+}cMSCs post-AMI. (A) Representative image of Periostin expression in heart tissue of the LV at 7 days post-AMI with or without neutralizing antibody administration (20μg/ml, AF2955, R&D systems), as analyzed by immunohistochemical (IHC) staining. Scale bars, 50 μm. **(B)** The expression level of Periostin in heart tissue of the LV at 7 days post-AMI was also analyzed by ELISA (ab193727, Abcam); n=4. **(C)** The survival rate was analyzed in mice subjected to Nes^{+}cMSCs treatment followed by the specific neutralizing antibody-mediated depletion of Periostin; n=15-30. **(D)** Heart function was evaluated by echocardiography at 3 weeks post-AMI, and LVEF and LVFS were measured; n=10-15. **(E and F)** Five heart sections (1-mm-thick) from each group were stained with 1% TTC for visualization of the infarct area (pale) and the viable myocardial area (brick red). Scale bars, 10 mm (E). Comparison of the relative scar areas among the study groups. The ratio of the length of the infarct band to the total length of the LV was calculated; n=5. (F). **(G and H)** The CD68^{+}CD206^{+} M2 macrophages in the infarcted areas at 7 days post-AMI were determined under fluorescence microscopy (G). Scale bars, 20 μm. The percentage of CD68^{+}CD206^{+} M2 macrophages was calculated using a double-blind method (H). Data are shown as mean ± SEM; n=5. *P <0.05, and ***P <0.001. Ab indicates the Periostin-neutralizing antibody.

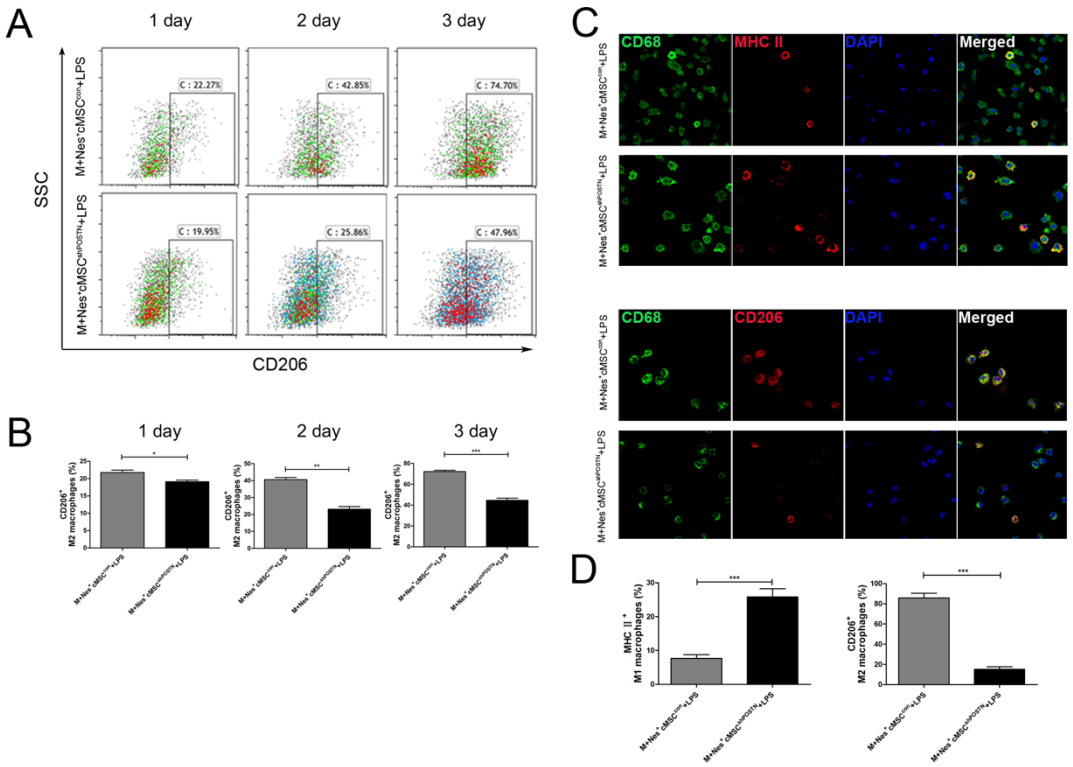

Figure S11. The down-regulation of Nes^{+}cMSC-secreted POSTN inhibits the polarization of M2 macrophages in vitro. (A and B) The percentage of CD68^{+}CD206^{+} M2 macrophages was analyzed by flow cytometry after macrophages were co-cultured for 1, 2, and 3 days with Nes^{+}cMSC^{con} or Nes^{+}cMSC^{shPOSTN}; n=3. **(C and D)** CD68^{+}MHCII^{+} M1 macrophages and CD68^{+}CD206^{+} M2 macrophages were examined by IF staining after 3 days of co-culture with Nes^{+}cMSC^{con} or Nes^{+}cMSC^{shPOSTN}, and percentages were calculated. Scale bars, 20 μm; n=3. Data are shown as mean ± SEM; n=3. *P <0.05, **P <0.01, and ***P <0.001.